

PAPER DETAILS

TITLE: Thermodynamic Analysis of an Intercity Bus Air-Conditioning System Working with HCFC, HFC, CFC and HC Refrigerants

AUTHORS: Mehmet BILGILI, Ediz CARDAK, Arif Emre AKTAS, Fırat EKİNCİ

PAGES: 29-43

ORIGINAL PDF URL: <https://dergipark.org.tr/tr/download/article-file/719688>



e-ISSN: 2146 - 9067

International Journal of Automotive Engineering and Technologies

journal homepage: <http://ijaet.academicpaper.org>



Original Research Article

Thermodynamic Analysis of an Intercity Bus Air-Conditioning System Working with HCFC, HFC, CFC and HC Refrigerants



Mehmet Bilgili¹, Ediz Cardak², Arif Emre Aktas^{2*}, Fırat Ekinci³

¹ Department of Mechanical Engineering, Ceyhan Engineering Faculty, Cukurova University, Adana, Turkey

² Department of Automotive Engineering, Engineering Faculty, Cukurova University, Adana, Turkey

³ Department of Energy System Engineering, Faculty of Engineering, Adana Alparslan Türkeş Science and Technology University, Adana, Turkey

ARTICLE INFO

ABSTRACT

* Corresponding author
aeaktas@cu.edu.tr,
arifemak@gmail.com

Received: January 25, 2019
Accepted: May 17, 2019

Published by Editorial Board
Members of IJAET

© This article is distributed by
Turk Journal Park System
under the CC 4.0 terms and
conditions.

The purpose of this study is to perform thermodynamic analysis of an intercity bus air-conditioning (ICBAC) system working with hydrochlorofluorocarbon (HCFC), hydrofluorocarbon (HFC), chlorofluorocarbon (CFC) and hydrocarbon (HC) refrigerants. For this aim, an intercity bus with a busload of 56 passengers, which is thought to motion in the Adana province of Turkey, was selected. R404A, R410A, R502, R507, R22, R290, R134a, R500 and R600a were selected as different HCFC/HFC/CFC/HC refrigerant types in the ICBAC system. Useful and reversible works of compressor, coefficient of performance (COP), exergy efficiency and exergy destructions of the entire ICBAC system and its each sub-unit were obtained. The results showed that the performance of the ICBAC system was significantly influenced by changing the refrigerants. However, R600a refrigerant based on hydrocarbon was found as a refrigerant to have minimum total exergy destruction, maximum exergy efficiency and maximum COP compared to other refrigerants used in the ICBAC system with the same amount of cooling load and the same climatic condition.

Keywords: Air-conditioning, Refrigerants, Air mixing ratios (MR), Exergy, Exergy efficiency, Intercity bus

1. Introduction

In recent years, global energy demand has shown an increase depending on the emerging technology, population growth, progress of living standards and industrialization of developing countries. At the same time, unfortunately, fossil fuels have been sharply declining, and worldwide energy related CO₂ emissions have been increasing [1-3]. Total energy demand is expected to increase about 21% by the year of 2030. Along with the

growing concern about climate change, in this context, governments around the world are requiring authorities to investigate alternative methods and thus to prevent emissions that cause greenhouse and other ecological effects [4].

Unless current policies change, the International Energy Agency (IEA) estimates that by 2030, worldwide energy-related CO₂ emissions will increase by about 50% compared to current levels. In addition, a 40% increase in oil demand will occur [5]. Fossil fuels will stay as

predominant by meeting 84% of the world's incremental energy needs. By the year of 2050, energy-based production of CO₂ is projected to be more than double, and concerns over the security of supplies will be heightened by the increased oil demand [6]. In the IEA Energy Technology Perspectives Baseline scenario 2015, CO₂ emissions will increase from 35.9 Gt in 2014 to 42 Gt by 2030. Growth in CO₂ emissions will continue in this scenario, and CO₂ emissions will probably reach 57 Gt in the year of 2050 [7]. In order to solve these two problems, researchers are focused on two solution proposals: (i) developing alternative energy sources (especially renewable energy sources) and (ii) improving energy efficiency [4].

Transportation technology is an essential component of economic progress and human prosperity. Besides, this technology is constantly developing as economies [8-9]. Parallel to this development, Air-Conditioning (AC) systems have great importance in transportation and other fields [10-14]. Regardless of the type of vehicle, the AC systems in the automotive sector often offer a number of advantages. Especially when the severe temperatures in Turkey are considered during summer, air conditioning systems are one of the indispensable comfort requirements for trucks, heavy duty machines, personal vehicles, city and intercity buses. However, the demand for the AC systems has led to a large amount of energy demand. Most air conditioners cannot be efficient for energy conservation and can consume large amounts of energy [15]. Generally, a more efficient automotive AC system can decrease fuel consumption, thus lower carbon emissions. This low emission technology is a fundamental subject of research on energy-efficient systems [8, 16]. For this reason, it is very important to ensure that the AC systems are controlled more effectively and to study on improving the energy efficiency of air conditioners.

It can be clearly seen that industrial revolution enhances the utilization of novel technological products in our daily life. In this regard the world energy demand increases rapidly and is expected to keep increasing in the foreseeable future. With the increasing demands, efficiency becomes more important in all industries

including public transportation day by day. Buses are one of the most important figures of public transportation [17]. They are designed to carry many passengers. In addition, the comfort of the passengers is as important as the energy efficiency. Optimum refrigerant must be selected for AC system to reduce energy consumption and increase passenger comfort. It is known that there are several available refrigerants for air-conditioning systems. R404A, R410A, R502, R507, R407C, R22, R290, R134a, R500 and, R600a are some of them. All of them have some small differences that matters to manufacturers. R134a and R600a are commonly used examples of these refrigerants.

Energy efficiency is one of the most substantial parameters of the energy generation technologies, and its policy is to reduce energy bills, to handle climate change and air pollution, to foster energy security, and to expand energy access. Exergy is the determination of the maximum useful work which can be extracted from any system. It has an important role in the development of strategies, the provision of guidelines for the efficient use of energy in thermal systems. Thus, it has become more essential investigation study than energy in order to determine the useful work [18-19].

There are various studies on energy efficiency and exergy analysis related to bus air conditioning system. Mansour et al. [20] studied a novel control strategy to enhance energy efficiency of a bus AC system operated in hot humid areas. Their study showed that the adopted control strategy increases the energy efficiency and thermal comfort on many partial load scenarios compared to the existing systems. Their economic analysis showed that system life cost would be reduced by 20% with the proposed system. Mansour et al. [21] performed a thermoeconomic optimization of a bus AC system equipped with a finned-tube evaporator configuration. Their study included the examining the effects of the chosen parameters on the evaporator configuration design. The study showed that a remarkable improvement could be achieved with the proposed design parameters compared to the currently used finned-tube evaporator. Shek and Chan [22] analyzed an integrated thermal comfort and air quality model of bus AC systems. In their study,

it can be concluded that the developed model could help to optimize AC control by creating an important balance between passengers comfort and energy efficiency. Direk and Hosoz [23] examined the energy and exergy analysis of a heat pump system for automotive application operating with R134a. In their study, it has been shown that automotive heat pump can be employed to supplement the primary comfort heating system of a vehicle that generates inefficient waste heat.

Alkan and Hosoz [24] performed an experimental study on automotive AC system equipped with a variable capacity compressor using different mechanical instruments. They found that increase in compressor speed leads to decrease in coefficient of performance (COP), whereas increase in exergy destruction and cooling capacity. Alkan and Hosoz [25] implemented an experimental study on exergy analysis of automotive AC system operating under variable and fixed capacity compressors. They showed in their study that the automotive AC system with variable capacity compressor has higher value of COP than the system with fixed capacity compressor. Furthermore, they expressed that increasing compressor speed of the fixed capacity compressor yields increase in total exergy destruction. Schulze et al. [26] performed a transient evaluation of a city bus AC system using R445a as a refrigerant. In their study, a method was presented to obtain the thermophysical properties of the R445a blend. Unal [27] used a two-phase ejector as an expansion device to raise the performance of a bus AC system. In their thermodynamic analysis, optimum overall lengths of two phase ejectors were calculated as 793.1 mm and 480.8 mm for the bus and midibus, respectively.

Yilmaz [28] developed transcritical organic Rankine cycle powered vapor compression refrigeration system for intercity bus AC operating with engine exhaust waste heat. In his study, dry refrigerant R245fa and wet refrigerant R134a were considered as refrigerants. It was found that cooling load of 30 kW for an intercity bus using proposed system can be achieved utilizing engine exhaust waste heat energy. Unal and Yilmaz [29] presented the thermodynamic analysis of a bus AC system with two-phase ejector as an expansion device. Their study showed that 15%

COP improvement can be achieved by using two phase ejector. Tosun et al. [30] conducted an exergy analysis to improve the performance of an intercity bus AC system. In their study, hourly cooling load capacity was obtained with HAP software after the number of passengers and meteorological data were determined. It was shown that performance of the AC system was significantly affected by the air mixing ratio and the outside air temperature. Exergy destruction values were calculated as 6.96 kW, 2.61 kW, 2.78 kW, 0.99 kW and for the compressor, condenser, evaporator and expansion valve, respectively.

In this study, thermodynamic analyses of an intercity bus AC (ICBAC) system were performed with different refrigerants. R404A, R410A, R502, R507, R22, R290, R134a, R500 and R600a were selected as different refrigerant types in the ICBAC system. An intercity bus with a busload of 56 people, which is thought to motion in the Adana province of Turkey, was selected. HAP is used to calculate hourly cooling load capacity of the intercity bus based on climatic data. Useful and reversible works of compressor, coefficient of performance (COP), exergy efficiency and destructions of entire ICBAC system and its each sub-unit was obtained and evaluated in a detailed way.

2. Material and Methods

2.1. Heat Gain Analysis

Calculation of heat gain (cooling load) is essential to design and determine the components of the HVAC system. Each heat gain realized by an intercity bus under defined conditions must be considered for cooling load design. The total generated cooling load is originated by equipment, appliances, passengers and lights, and transferred heat through the intercity bus wrap, including front and rear bodies, side panels, ceiling, windows, doors, floor etc. The heat transfers from opaque surfaces, some of which are front, rear, roof, side and floor panels, can be calculated as [30]:

$$\dot{Q}_{opaque} = U_{opaque} \cdot A_{opaque} \cdot CLTD \quad (1)$$

where A_{opaque} and U_{opaque} are the heat transfer surface area of the overall side panel of the intercity bus and the total heat transfer coefficient, respectively. CLTD is the abbreviation for the temperature difference of

cooling load. Moreover, the rate of heat transfer from glass can be calculated as [30]:

$$\dot{Q}_{glass} = A_{glass} \cdot U_{glass} \cdot (T_o - T_i) + SHGF_{max} \cdot SC \quad (2)$$

Where A_{glass} , U_{glass} , T_o and T_i are glass area, glass heat transfer coefficient, the outdoor and indoor air temperature, respectively. Besides, $SHGF_{max}$ the abbreviation for maximum solar heat gain factor, and SC is the shading coefficient. The latent and sensible heat gains resulting from the bypass air ventilation are given by [30]:

$$\dot{Q}_{l,by-pass} = \dot{m}_o \cdot BF \cdot h_{fg} (w_o - w_i) \quad (3)$$

$$\dot{Q}_{s,by-pass} = \dot{m}_o \cdot BF \cdot c_p (T_o - T_i) \quad (4)$$

Where, \dot{m}_o , c_p and BF are outdoor air mass flow rate, specific heat of moist air and bypass factor, respectively. The latent heat of vaporization is denoted as h_{fg} . Moreover, w_o and w_i are the outdoor and indoor air humidity ratios, respectively. There are also inertial loads resulting from passengers, equipment, appliances and lighting as well as those external loads. Lastly, the latent cooling load, $\dot{Q}_{l,bus}$, the sensible cooling load, $\dot{Q}_{s,bus}$, and total cooling load, $\dot{Q}_{total,bus}$, of the intercity bus can be calculated as [30]:

$$\dot{Q}_{l,bus} = \dot{Q}_{l,by-pass} + \dot{Q}_{l,infiltration} + \dot{Q}_{l,occupants} + \dot{Q}_{l,appliances} \quad (5)$$

$$\dot{Q}_{s,bus} = \dot{Q}_{s,glass} + \dot{Q}_{s,opaque} + \dot{Q}_{s,by-pass} + \dot{Q}_{s,infiltration} + \dot{Q}_{s,occupants} + \dot{Q}_{s,appliances} + \dot{Q}_{s,lighting} \quad (6)$$

$$\dot{Q}_{total,bus} = \dot{Q}_{s,bus} + \dot{Q}_{l,bus} \quad (7)$$

2.2. AC System Analysis

The ICBAC system is illustrated in Figure 1. As shown, the outside fresh air is firstly mixed with recirculated air to satisfy the ventilation requirement. Then, the mixed air flows through the cooling coil (evaporator), and it is supplied to the cabin by the evaporator fan. A standard ICBAC unit includes compressor, evaporator expansion valve and condenser. The system generally uses an open drive compressor

connected to the bus engine with a belt. An electrically controlled clutch which creates engagement between the compressor pulley and compressor drive shaft to supply required amount of air to the AC system.

Outdoor air mass flow rate, \dot{m}_o , and indoor air mass flow rate, \dot{m}_i , are mixed at a constant pressure and certain rate. The air mixing ratio, MR is given by:

$$MR = \frac{\dot{m}_o}{\dot{m}_i} \quad (8)$$

The mass balance and energy balance must be taken into account to obtain the mixed air mass flow rate, \dot{m}_s , and its thermodynamic properties. Mass flow rates of dry air and water vapor can be calculated as:

$$\dot{m}_s = \dot{m}_o + \dot{m}_i \quad (9)$$

$$\dot{m}_m w_m = \dot{m}_o w_o + \dot{m}_i w_i \quad (10)$$

From the energy balance:

$$\dot{m}_s h_s = \dot{m}_o h_o + \dot{m}_i h_i \quad (11)$$

$\dot{Q}_{l,bus}$ and $\dot{Q}_{s,bus}$ of the intercity bus are given by:

$$\dot{Q}_{l,bus} = \dot{m}_s \cdot h_{fg} (w_i - w_o) \quad (12)$$

$$\dot{Q}_{s,bus} = \dot{m}_s \cdot c_p (T_i - T_o) \quad (13)$$

Bypass factor, BF can be calculated as:

$$BF = \frac{T_s - T_{ADP}}{T_m - T_{ADP}} \quad (14)$$

where T_s , T_{ADP} and T_m are the supply air, the coil apparatus dew-point and the mixed air temperatures, respectively. The optimum capacity of the cooling coil, \dot{Q}_{eva} can be obtained as follows:

$$\dot{Q}_{eva} = \dot{m}_s (h_m - h_s) + \dot{m}_w h_w \quad (15)$$

Where h_w and \dot{m}_w are the enthalpy of condensate exiting the cooling coil (evaporator) and condensed water mass flow rate passing through the coil, respectively. \dot{m}_w can be calculated as follows:

$$\dot{m}_w = \dot{m}_s (w_i - w_s) \quad (16)$$

2.3. Refrigeration System Analysis

Energy balance of steady-state operation is given as:

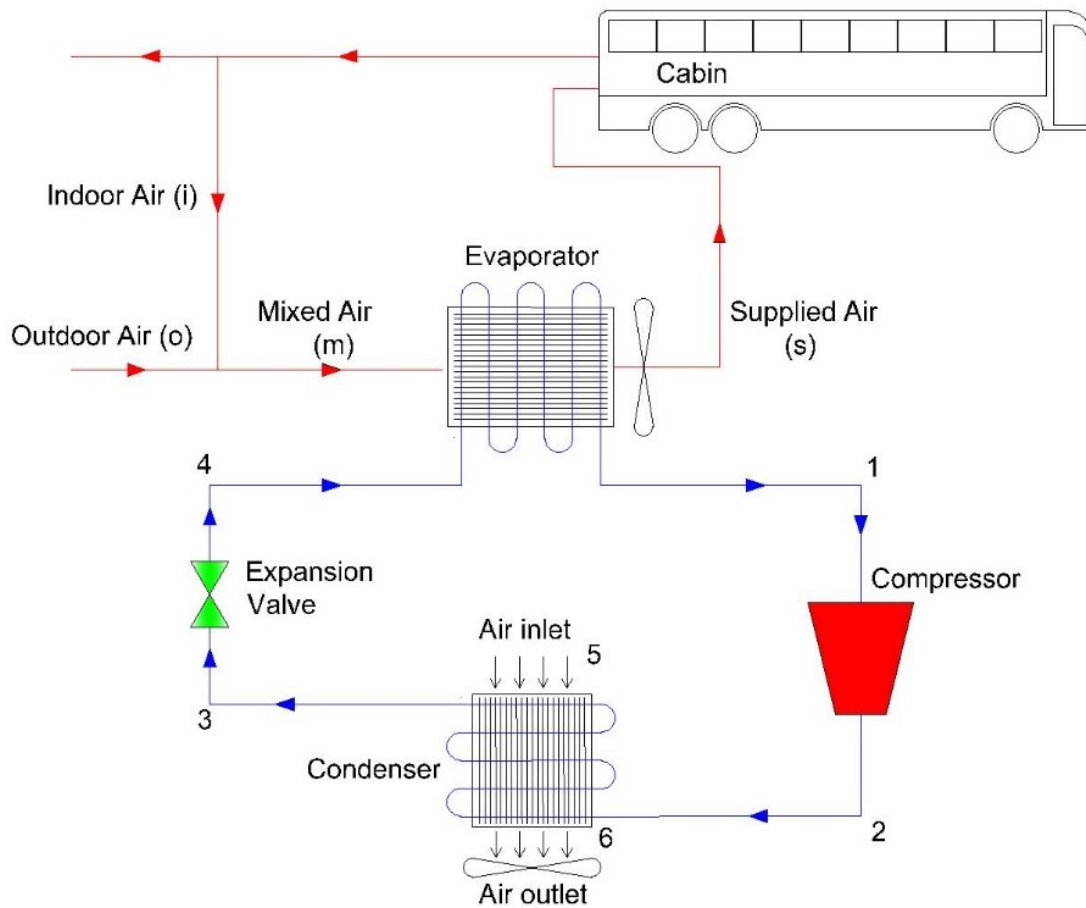


Figure 1. Schematic view of the intercity bus air conditioning system

$$\dot{L}_{in} - \dot{L}_{out} \quad (17)$$

where the \dot{L}_{in} and \dot{L}_{out} are the rate of net energy entering and leaving the control volume in the form of heat, \dot{Q} , work, \dot{W} , and mass, \dot{m} , respectively. In general, energy balance equation for steady-flow process is defined as [31];

$$\dot{Q}_{in} - \dot{Q}_{out} - \dot{W}_{out} = \dot{m} \left(\frac{V^2}{2} + g \cdot z \right) \quad (18)$$

where h , V and z are the enthalpy, the system velocity with respect to an outside reference frame, and the vertical distance of the center of gravity of a system with respect to a chosen reference elevation, respectively. The enthalpy, h_2 at the outlet of the compressor is stated as [32];

$$h_2 = h_1 + \frac{h_{2s} - h_1}{\eta} \quad (19)$$

Where the specific enthalpy at state 2s is defined as h_{2s} . Compressor isentropic efficiency, η can

be calculated as [32];

$$\eta = 0.874 - 0.0135 \frac{P_{con}}{P_{eva}} \quad (20)$$

Here, P_{con} is the condenser pressure and P_{eva} is the evaporator pressure. Entropy balance equation can be written as [30];

$$\dot{L}_{gen} = \sum \frac{\dot{Q}_k}{T_k} \quad (21)$$

where \dot{L}_{gen} is the entropy generation, s is the entropy, T_k is the temperature at location k , and \dot{Q}_k is the amount of heat transfer across the boundary at location k . The exergy destruction, $\dot{E}x_{des}$ can be determined as [31];

$$\dot{E}x_{des} = T_o \dot{S}_{gen} \quad (22)$$

where T_o stands for dead-state temperature. Entropy change equation can be expressed as:

$$s_2 - s_1 = c_{p,avg} \cdot \ln \frac{T_2}{T_1} - R \ln \frac{P_2}{P_1} \quad (23)$$

The general exergy balance is written as:

$$\dot{E}x_{in} - \dot{E}x_{out} - \dot{E}x_{des} \quad (24)$$

Where the difference $\dot{L}_{in} - \dot{L}_{out}$ is the net

exergy transfer rate by work, heat and mass. Moreover, the net exergy destruction rate is indicated with $\dot{E}x_{des}$ in the equation above. The exergy balance equation can define as:

$$\dot{L}_{heat} + \dot{L}_{work} + \dot{L}_{mass,in} = \dot{L}_{mass,out} + \dot{L}_{des} \quad (25)$$

The exergy balance equation can be written in the following form:

$$\sum \left(1 - \frac{T_0}{T_k}\right) \cdot \dot{Q}_k + \dot{W} = \dot{L}_{des} \quad (26)$$

$$\sum (\dot{E}x_{in}) = \dot{L}_{des}$$

Where \dot{W} and ex are the work rate and the flow (specific) exergy, respectively. Additionally, the properties at the dead state of P_0 and T_0 are shown as subscript zero. The specific flow exergy is expressed as [30]:

$$ex = (h - h_0) - T_0 \cdot (s - s_0) \quad (27)$$

The exergy rate is calculated as [33]:

$$\dot{L}_{des} = \dot{E}x_{des} \quad (28)$$

The exergy efficiency, ψ can be calculated as:

$$\psi = \frac{\dot{L}_{out} - \dot{L}_{in}}{\dot{L}_{in}} = \frac{\text{exergy recovered}}{\text{exergy supplied}} \quad (29)$$

The coefficient of performance, COP which is used to quantify the performance of the refrigeration cycle can be determined from the following ratio:

$$COP = \frac{\dot{Q}_{eva}}{\dot{W}_{comp}} \quad (30)$$

The reversible power, \dot{W}_{rev} is the minimum required power for the compressor, and it can be written as:

$$\dot{W}_{rev} = \dot{L}_{comp} - \dot{L}_{des} - \dot{L}_{out,comp} + \dot{L}_{in,comp} \quad (31)$$

The obtained equations of mass, energy, entropy, exergy balance and exergy efficiency for each component of the ICBAC system are given in Table 1.

3. Results and Discussions

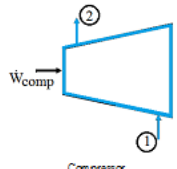
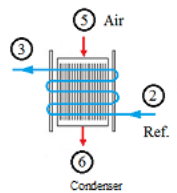
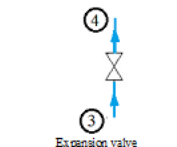
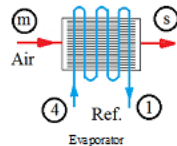
3.1. Study Region, Climatic Data, Properties and Dimensions of the Intercity Bus

As the study region where the work will be done, the Adana province of Turkey was chosen. Climate data such as dry bulb temperature, wet bulb temperature and solar

radiation of the Adana province were used in order to determine the cooling load of the intercity bus.

Selected bus for this research with a busload of 56 passengers which is used for intercity transport. Figure 2 illustrates the schematic view and dimensions of the intercity bus. The intercity bus with an integral body structure is framed from stainless steel ensuring strength and stability. The material properties such as total heat transfer coefficient and shade coefficient of the intercity bus are given in Table 2.

Table 1. Mass, energy, entropy, exergy balances and exergy efficiency for the ICBAC system components

Component and schematic view	Description	Formula
 Compressor	Mass Balance	$\dot{m}_1 = \dot{m}_2 = \dot{m}_{ref}$
	Energy Balance	$\dot{W}_{comp} = \dot{m}_{ref} \cdot (h_2 - h_1)$
	Entropy Balance	$\dot{S}_{gen,comp} = \dot{m}_{ref} \cdot (s_2 - s_1)$
	Exergy Balances	$\dot{E}x_{des,comp} = \dot{m}_{ref} \cdot (ex_2 - ex_1) + \dot{W}_{comp}$
	Exergy Efficiency	$\psi_{comp} = \frac{\dot{E}x_2 - \dot{E}x_1}{\dot{W}_{comp}}$
	Mass Balance	$\dot{m}_2 = \dot{m}_3 = \dot{m}_{ref}; \dot{m}_5 = \dot{m}_6 = \dot{m}_{air}$
 Condenser	Energy Balance	$\dot{Q}_{con} = \dot{m}_{ref} \cdot (h_2 - h_3) = \dot{m}_{air} \cdot c_{p,air} \cdot (T_6 - T_5)$
	Entropy Balance	$\dot{S}_{gen,con} = \dot{m}_{ref} \cdot (s_3 - s_2) + \dot{m}_{air} \cdot \left(c_{p,air} \cdot \ln \frac{T_6}{T_5} - R \cdot \ln \frac{P_6}{P_5} \right)$
	Exergy Balances	$\dot{E}x_{des,con} = \dot{m}_{ref} \cdot (ex_2 - ex_3) + \dot{m}_{air} \cdot (ex_5 - ex_6)$
	Exergy Efficiency	$\psi_{con} = \frac{\dot{m}_{ref} \cdot (ex_2 - ex_3)}{\dot{m}_{ref} \cdot (ex_2 - ex_3)}$
	Mass Balance	$\dot{m}_3 = \dot{m}_4 = \dot{m}_{ref}$
	Energy Balance	$\dot{h}_3 = \dot{h}_4$
 Expansion valve	Entropy Balance	$\dot{S}_{gen,exp.val} = \dot{m}_{ref} \cdot (s_4 - s_3)$
	Exergy Balances	$\dot{E}x_{des,exp.val} = \dot{m}_{ref} \cdot (ex_3 - ex_4)$
	Exergy Efficiency	$\psi_{exp.val} = \frac{\dot{m}_{ref} \cdot (ex_3)}{\dot{m}_{ref} \cdot (ex_3)}$
	Mass Balance	$\dot{m}_1 = \dot{m}_4 = \dot{m}_{ref}; \dot{m}_m = \dot{m}_5 = \dot{m}_{air}$
	Energy Balance	$\dot{Q}_{eva} = \dot{m}_{ref} \cdot (h_1 - h_4) = \dot{m}_s \cdot (h_m - h_s) - \dot{m}_w \cdot h_w$
	Entropy Balance	$\dot{S}_{gen,eva} = \dot{m}_{ref} \cdot (s_1 - s_4) + \dot{m}_{air} \cdot \left(c_{p,air} \cdot \ln \frac{T_1}{T_m} - R \cdot \ln \frac{P_1}{P_m} \right)$
 Evaporator	Exergy Balances	$\dot{E}x_{des,eva} = \dot{m}_{ref} \cdot (ex_4 - ex_1) + \dot{m}_{air} \cdot (ex_m - ex_s)$
	Exergy Efficiency	$\psi_{evaporator} = \frac{\dot{m}_{ref} \cdot ex_1 + \dot{m}_{air} \cdot ex_s}{\dot{m}_{ref} \cdot ex_4 + \dot{m}_{air} \cdot ex_m}$
	Exergy Efficiency	$\psi_R = \frac{\dot{E}x_{in,eva} - \dot{E}x_{out,eva}}{\dot{W}_{comp}}$
	Total exergy Destruction	$\dot{E}x_{des,total} = \dot{E}x_{des,comp} + \dot{E}x_{des,cond} + \dot{E}x_{des,exp.val} + \dot{E}x_{des,eva}$
Refrigeration unit		

3.2. Cooling Load Capacity of Intercity Bus

In order to determine the hourly cooling load capacity of the intercity bus, Hourly Analysis Program (HAP) was used. Table 3 gives details of latent and sensible loads on the intercity bus.

Table 2. The material properties such as total heat transfer coefficient and shade coefficient of the intercity bus [30, 34]

Material	Total heat transfer coefficient (W/m ² .K)	Shade coefficient
Side panel	2.801	-
Front panel	2.667	-
Rear panel	2.667	-
Floor	2.667	-
Roof	0.532	-
Side window	2.569	0.811
Front window	5.020	0.811
Rear window	2.611	0.811
Door window	4.890	0.811
Skylight	4.890	0.811

In the cooling load determination, it was assumed that the intercity bus was traveling in the direction of south to north with a speed of 120 km/h. It was considered that heat transfer from the windows as a sensible heat gain takes place by radiation and conduction, while heat transfer from the ceiling, floor, front, rear and side panels is realized only by conduction. Due to its small amount, heat transfer by air leakage was ignored. In addition, latent and sensible heat gains from passengers, devices and bypass ventilation air were determined, and hence the total cooling load on the intercity bus was calculated. Figure 3 demonstrates the total cooling load on the intercity bus as a function of hours of the day and given months.

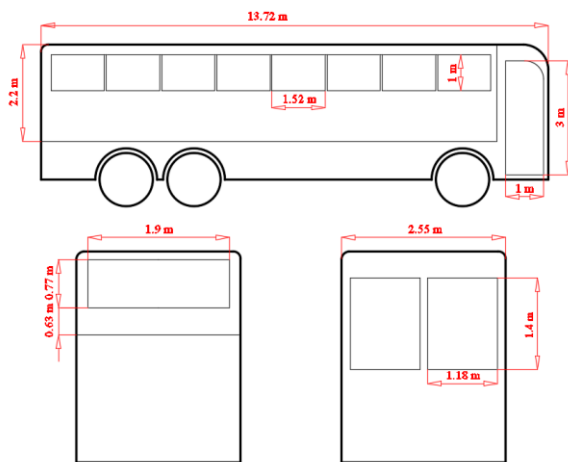


Figure 2. Schematic view and dimensions of the intercity bus [34]

As shown in the figure, alteration in atmospheric air temperature and solar radiation causes remarkable variation in the total cooling load (heat gain) of the intercity bus throughout the day. For example, the maximum value of heat gain was determined to be roughly 26 kW at about 17:00. The minimum value of heat gain

was obtained at times when outside ambient air temperature and solar radiation are low. The highest value of cooling load was found almost as 26 kW at about 17:00 in July month and this condition is the peak cooling load and peak time. As the traveling direction of the bus is South to North, radiation values emitted from the side windows reaches the highest value on July 23 at 17:00 [35].

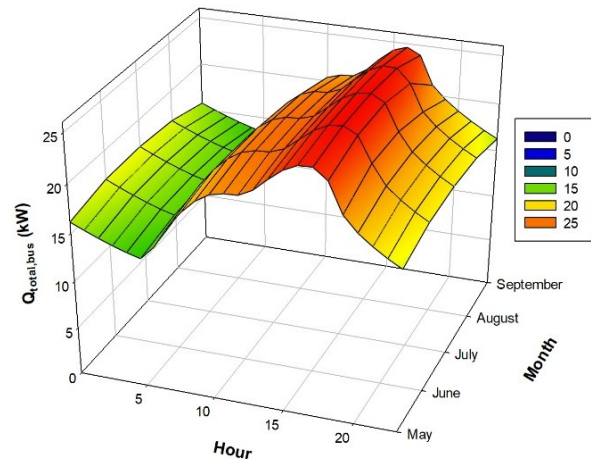


Figure 3. Hourly total cooling load variation on the intercity bus for different months

Table 3. Details of sensible and latent cooling loads on the intercity bus (Cooling design, outer area dry/wet bulb temperature: 36.8°C / 25.7°C, Air-conditioning space temperature: 24.4°C)

Load component	Detail	Sensible cooling load (W)	Latent cooling load (W)
Window and Skylight Loads	Solar 35 m ²	6162	-
Wall Transmission	28 m ²	1891	-
Roof Transmission	32 m ²	445	-
Window Transmission	34 m ²	1145	-
Skylight Transmission	1 m ²	42	-
Door Loads	0 m ²	0	-
Floor Transmission	33 m ²	796	-
Partitions	0 m ²	0	-
Ceiling	0 m ²	0	-
Overhead Lighting	0 W	0	-
Task Lighting	0 W	0	-
Electric Equipment	0 W	0	-
People Infiltration	56	3774	1971
People Infiltration	-	0	0
People Infiltration	56	3774	1971
People Infiltration	-	0	0
Miscellaneous	-	0	0
Safety Factor	60% / 60%	8553	1183
Total Zone Loads	-	22808	3154

3.3. Energy Analysis of the ICBAC System

In the previous section, the peak (maximum) cooling load was determined for the July month at about 17:00. Therefore, the energy and exergy analyzes of the ICBAC system were made considering the found peak load values. The air mixing ratio (MR) was considered to be 0.5. Accordingly, the determined inside and outside design conditions and the thermodynamic properties and characteristics of the ICBAC

system are given in Table 4. The ICBAC system with outdoor air for ventilation and the corresponding process on psychrometric diagram are demonstrated in Figure 4.

As seen from Figures 1 and 4, to meet the ventilation requirement, indoor air (i) is firstly mixed with outdoor air (o) at a certain mass flow rate. Then, the mixture air (m) flows over the cooling coil (evaporator), where it is cooled and dehumidified, and the air (s) is also provided to the conditioned space.

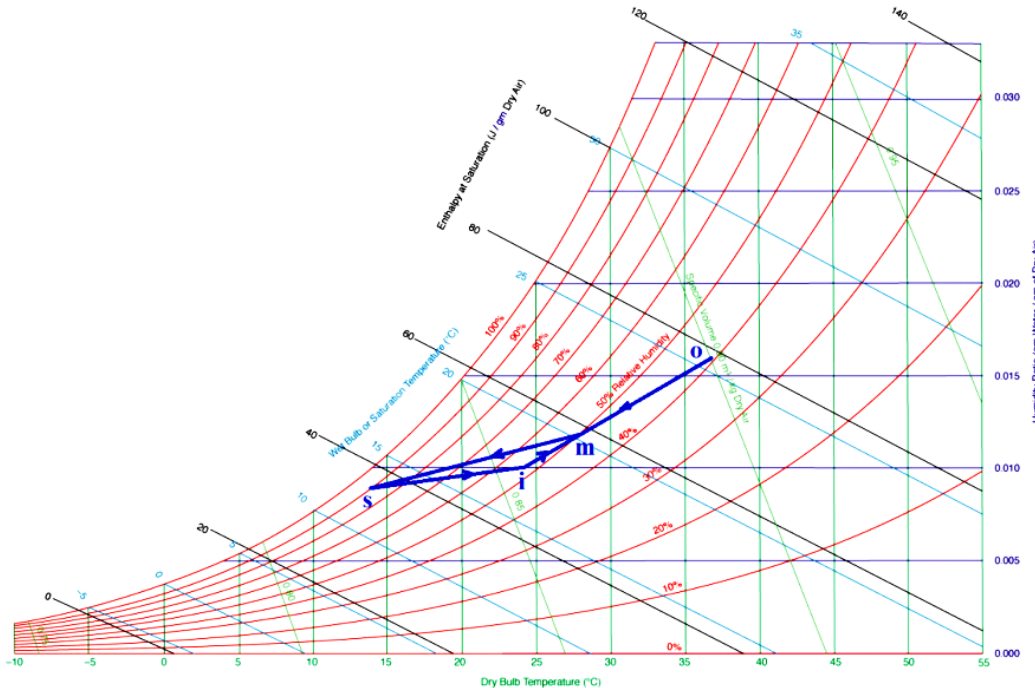


Figure 4. The ICBAC system with outdoor air for ventilation and the corresponding process on psychrometric diagram

The intercity bus cabin is maintained at 24.4°C dry bulb temperature with 50% relative humidity, while the outside design temperatures are 36.8°C dry bulb and 25.7°C wet bulb.

The outdoor air and the indoor air are mixed with a ratio of $MR = 0.5$ and, the mixing air temperature is found to be 28.53°C.

The supply air to the conditioned space is assumed to be 10°C lower than the inside temperature, and so it is determined as 14.4°C. By the way, since the bus sensible heat gain ($\dot{Q}_{s,bus}$) and the bus latent heat gain ($\dot{Q}_{l,bus}$) are 22.808 kW and 3.154 kW respectively, the mass flow (\dot{m}_s), bypass factor (BPF) and the apparatus dew point temperature (T_{ADP}) values are calculated as 2.233 kg/s, 0.2141 and 10.55°C, respectively. Moreover, the amount of heat transfers within the evaporator and the amount of condensation on the evaporator surface are calculated as 49.030 kW and

0.00654 kg/s, respectively.

R404A, R410A, R502, R507, R22, R290, R134a, R500 and R600a were selected as different refrigerant types in the ICBAC system. Table 5 lists physical, safety and environmental properties of those refrigerants based on literature survey. As an example, the pressure-enthalpy (P-h) diagram of the ICBAC system with refrigerant R134a is shown in Figure 5.

The thermodynamic properties of all refrigerants were obtained using the program known as CoolPack V2.85. Energy analysis results of the ICBAC system for a sample refrigerant (R600a) are given in Table 6. In the calculations of the refrigeration cycle, the value of the evaporation temperature of the refrigerant was considered to be equal to the apparatus dew point temperature.

The condensation temperature of the refrigerant was assumed as 15°C above the atmospheric air temperature. The superheated and subcooling

temperature values were taken as 10°C. Figure 6 illustrates the influence of different refrigerants on COP values of the ICBAC system and the compressor power input such as

Table 4. The determined inside and outside design conditions, the thermodynamic properties and characteristics of the ICBAC system

Properties	Unit	Value
Dry bulb temperature of indoor air, T_i	°C	24.4
Wet bulb temperature of indoor air, $T_{i,wb}$	°C	17.4
Specific humidity of indoor air, w_i	kg/kg	0.00953
Enthalpy of indoor air, h_i	kJ/kg	48.82
Dry bulb temperature of outdoor air, T_o	°C	36.8
Wet bulb temperature of outdoor air, $T_{o,wb}$	°C	25.7
Specific humidity of outdoor air, w_o	kg/kg	0.01626
Enthalpy of outdoor air, h_o	kJ/kg	78.79
Sensible cooling load of the intercity bus, $\dot{Q}_{s,bus}$	kW	22.808
Latent cooling load of the intercity bus, $\dot{Q}_{l,bus}$	kW	3.154
Total cooling load of the intercity bus, $\dot{Q}_{total,bus}$	kW	25.962
Enthalpy of condensate water, h_w	kJ/kg	60.982
Dry bulb temperature of supply air, T_s	°C	14.4
Enthalpy of supply air, h_s	kJ/kg	36.67
Specific humidity of supply air, w_s	kg/kg	0.00884
Dry bulb temperature of mixed air, T_m	°C	28.53
Specific humidity of mixed air, w_m	kg/kg	0.01177
Enthalpy of mixed air, h_m	kJ/kg	58.810
Mass flow rate of supply air, \dot{m}_s	kg/s	2.233

useful power and reversible power. As seen from the figure, minimum compressor powers and maximum COP values were calculated for refrigerant R600a, while maximum compressor powers and minimum COP values were obtained for refrigerant R404A. For example, the useful power input and reversible power values for refrigerant R404A were found as 10.99 kW and 9.35 kW, respectively, while for the R600a refrigerant these values were calculated as 9.57 kW and 8.08 kW, respectively.

The reversible power of 8.08 kW is the minimum required power for the compressor of the ICBAC system. On the other hand, COP value was 4.46 for refrigerant R404A, while for refrigerant R600a this value reached 5.13 with an increase of 15%. Therefore, the most effective refrigerant obtained for the ICBAC system was R600a in terms of low compressor power input and high COP. Figure 7 shows the heat transfer values in the condenser and evaporator for studied refrigerants. As observed in the figure, the difference between the heat transfer values in the condenser and the evaporator decreased when the refrigerant was changed from R404A to R600a.

For example, the heat transfer difference was obtained as 10.99 kW for the R404A refrigerant, while for the R600a refrigerant this difference was calculated as 9.57 kW. This means that the compressor with refrigerant R600a systems consumes 10.12% less energy than refrigerant R404A systems.

Table 5. The properties of working fluids

Refrigerant	Chemical Formula	Physical Data			Safety Data		Environmental Data	
		M (g/mol)	P _c (MPa)	T _c (°C)	LFL (%)	Safety Group	ODP	GWP (100 yr)
R404A	CHF ₂ CF ₃ /CH ₂ CF ₃ /CH ₂ FCF ₃ ^a	97.60 ^a	3.731 ^a	72.07 ^a	none	A1 ^b	0 ^c	3800 ^c
R410A	CH ₂ F ₂ + CHF ₂ CF ₃ ^b	72.60	4.901 ^d	71.3 ^d	none ^b	A1 ^b	0 ^c	2000 ^c
R502	CHClF ₂ + CClF ₂ CF ₃ ^b	111.6 ^b	4.019 ^c	80.73 ^c	none ^b	A1 ^c	0.221 ^c	4500 ^c
R507	CHF ₂ CF ₃ + CH ₃ CF ₃ ^b	98.9 ^b	3.716 ^b	70.5 ^b	none ^b	A1 ^b	0 ^b	3985 ^b
R22	CHClF ₂ ^c	86.47 ^f	4.99 ^f	96.15 ^f	none ^b	A1 ⁱ	0.055 ^c	1700 ⁱ
R290	C ₃ H ₈	44.10 ^g	4.25 ^g	96.7 ^g	2.1 ^g	A3 ^g	0.0 ^h	~20 ^h
R134a	CH ₂ FCF ₃ ^c	102.03 ^f	4.06 ^f	101.05 ^f	none ^b	A1 ⁱ	0.0 ⁱ	1300 ⁱ
R500	CCl ₂ F ₂ + CHF ₂ CH ₃ ^b	99.31 ^b	4.172 ^b	102.1 ^b	none ^b	A1 ^b	0.66 ^b	8077 ^b
R600a	Iso-C ₄ H ₁₀ ^g	58.12 ^g	3.63 ^g	134.7 ^g	1.6 ^g	A3 ^g	0.0 ^h	~20 ^h

^a Ref.[36], ^b Ref.[37], ^c Ref.[38], ^d Ref.[39], ^e Ref.[40], ^f Ref.[41], ^g Ref.[42], ^h Ref.[43], ⁱ Ref.[44]

3.4. Exergy Analysis of ICBAC System

In the analysis of intercity bus air-conditioning system, the dead-state temperature (T_0) is assumed as the outside ambient temperature, 36.8°C in July month. The humid specific heat

of moist air, $C_{p,air}$ is taken as 1.0216 kJ/kg-dry-air.K. Besides, the dead-state pressure (P_0) is assumed as 101.325 kPa. Energy analysis results of the ICBAC system for a sample refrigerant (R134a) are given in Table 7.

Figure 8 presents the exergy destruction values for the compressor, evaporator, condenser and expansion valve equipment of the ICBAC system according to different refrigerants. As can be seen from the figure, for all refrigerants,

the highest exergy destruction value was obtained at the evaporator. However, the lowest exergy destruction value was acquired at the expansion valve except for refrigerant R404A.

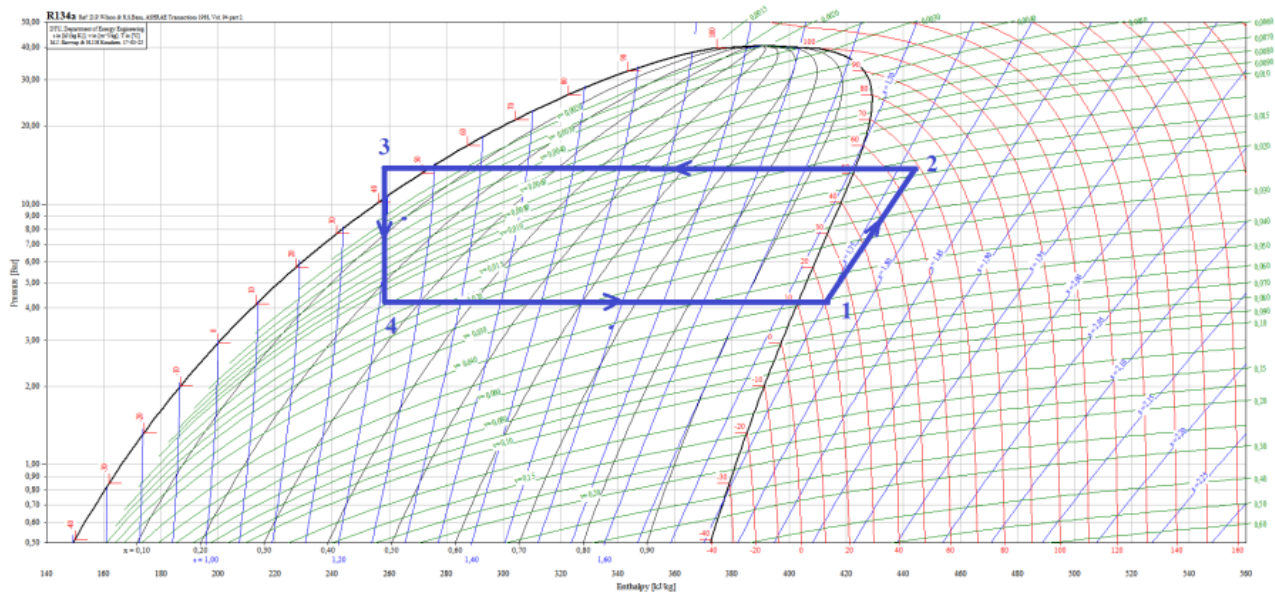


Figure 5. The pressure-enthalpy (P-h) diagram of the ICBAC system with the R134a refrigerant

Table 6. Energy analysis results of the ICBAC system for a sample refrigerant (R600a)

Properties	Unit	Value
Condenser pressure, P_1	kPa	225.9
Condensation temperature, T_c	°C	51.8
Evaporator pressure, P_2	kPa	732.2
Evaporation temperature, T_e	°C	10.55
Compressor inlet temperature of refrigerant, T_1	°C	20.55
Compressor outlet temperature of refrigerant, T_2	°C	59.88
Condenser outlet temperature of refrigerant, T_3	°C	41.8
Evaporator inlet temperature of refrigerant, T_4	°C	10.55
Mass flow rate of refrigerant, \dot{m}_{ref}	kg/s	0.1707
Mass flow rate of air in condenser, \dot{m}_a	kg/s	6.1831
Mass flow rate of air in evaporator, \dot{m}_s	kg/s	2.233
Condenser inlet temperature of air, T_5	°C	36.8
Condenser outlet temperature of air, T_6	°C	46.08
Compressor isentropic efficiency, η	%	0.8446
Enthalpy at the point 1, h_1	kJ/kg	586.888
Enthalpy at the point 2, h_2	kJ/kg	642.911
Enthalpy at the point 3, h_3	kJ/kg	299.734
Enthalpy at the point 4, h_4	kJ/kg	299.734
Entropy at the point 1, s_1	kJ/kg.K	2.3639
Entropy at the point 2, s_2	kJ/kg.K	2.3920
Entropy at the point 3, s_3	kJ/kg.K	1.3360
Entropy at the point 4, s_4	kJ/kg.K	1.3530
Entropy at the point 4, s_4	kJ/kg.K	1.3530
Heat transfer on the cooling coil, \dot{Q}_{cool}	kW	49.030
Mass flow rate of condensate water, $\dot{r}_{..}$	kg/s	0.00654
Apparatus dew point temperature, TADP	°C	10.55
Bypass factor, BPF	-	0.2141
Air mixing ratio, MR	-	0.5

Figure 9 shows the exergy efficiency values for the compressor, evaporator, condenser and expansion valve equipment of the ICBAC system as a function of different refrigerants. As observed in the figure, the lowest exergy efficiency values for all refrigerants were obtained from the condenser, while the highest exergy efficiency values were calculated in the expansion valve. It was concluded that if the refrigerant is changed from R404A to R600a, the values of exergy efficiency decrease considerably, especially in the evaporator.

The variation of overall exergy efficiency and total exergy destruction values of the ICBAC

system according to different refrigerants is illustrated in Figure 10. It is seen that; the total exergy destruction values decrease with replacing the R404A refrigerant with R600a on the ICBAC system. Besides, the overall exergy efficiency values of the ICBAC system increase prominently. For example, the total exergy destruction value is 8.4 kW for the ICBAC system with refrigerant R404A, while for the R600a refrigerant this value drops to 7.02 kW. This reduction of 1.38 kW in the total exergy destruction results in a 16.3% increases in the overall exergy efficiency value of the ICBAC system.

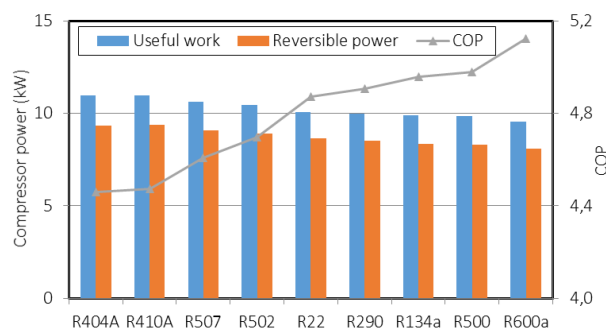


Figure 6. The effect of different refrigerants on the COP values and the compressor power input of the ICBAC system

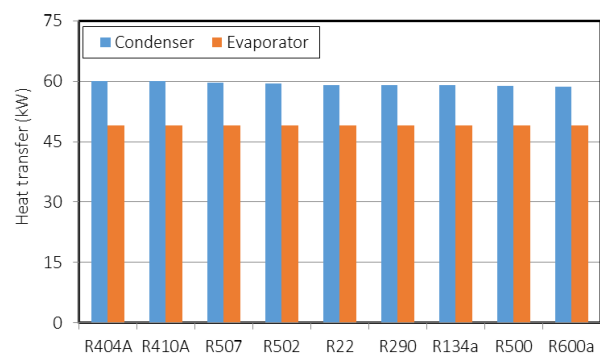


Figure 7. The heat transfers in the condenser and evaporator for different refrigerants

Table 7. Exergy analysis results of the system for a sample refrigerant (R134a)

SN	Description	Fluid	Phase	Temp. (°C)	Press. (kPa)	Enthalpy (kJ/kg)	Entropy (kJ/kgK)	Mass flow rate (kg/s)	Specific energy (kJ/kg)	Exergy rate (kW)
0	-	Air	Dead state	36.8	101.325	-	-	-	0	0
0	-	R134a	Dead state	36.8	101.325	434.73	1.934	-	0	0
1	Compressor inlet	R134a	Superheated vapor	20.55	4.222	412.893	1.750	0.3183	35.17	11.19
2	Compressor outlet	R134a	Superheated vapor	68.55	13.782	443.963	1.766	0.3183	61.28	19.51
3	Condenser outlet	R134a	Liquid	41.8	13.782	258.862	1.198	0.3183	52.15	16.60
4	Evaporator inlet	R134a	Mixture	10.55	4.222	258.862	1.208	0.3183	49.05	15.61
5	Condenser inlet	Air	Gas	36.8	101.325	-	-	6.1831	0	0
6	Condenser outlet	Air	Gas	46.13	101.325	-	-	6.1831	0.14	0.87
m	Evaporator inlet	Air	Gas	28.53	101.325	-	-	2.233	0.114	0.25
s	Evaporator outlet	Air	Gas	14.4	101.325	-	-	2.233	0.87	1.94

4. Conclusions

In this study, thermodynamic analyses were performed to enhance the efficiency of the ICBAC system. Typical refrigerants R404A, R410A, R502, R507, R22, R290, R134a, R500 and R600a were selected as different refrigerant types in the ICBAC system. The maximum value of heat gain was determined to be roughly 26 kW at about 17:00 in July month. Heat transfer value in the evaporator was calculated

as 49.030 kW. The most effective refrigerant for the ICBAC system was obtained as R600a in terms of low compressor power input and high COP. The COP value of the ICBAC system with refrigerant R404A was calculated as 4.46, while for refrigerant R600a this value was determined as 5.13. The lowest exergy efficiency values for all refrigerants were obtained from the condenser, while the highest exergy efficiency values were calculated in the expansion valve. The total exergy destruction values decreased

with replacing the R404A refrigerant with R600a on the ICBAC system. The total exergy destruction value was found as 8.4 kW for the ICBAC system with refrigerant R404A, while for the refrigerant R600a this value dropped to 7.02 kW. As a result, R600a has the highest overall exergy efficiency and lowest total exergy destruction among all studied refrigerants, while R404A has the lowest overall exergy efficiency and highest total exergy destruction.

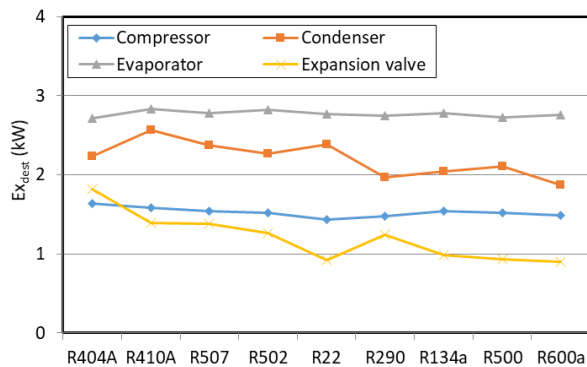


Figure 8. The exergy destruction values for the compressor, condenser, evaporator and expansion valve equipment of the ICBAC system

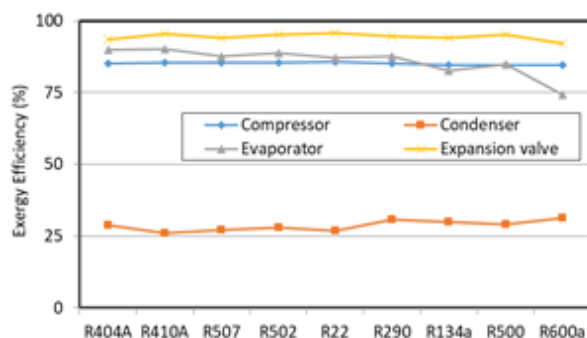


Figure 9. The exergy efficiency values for the compressor, condenser, evaporator and expansion valve equipment of the ICBAC system

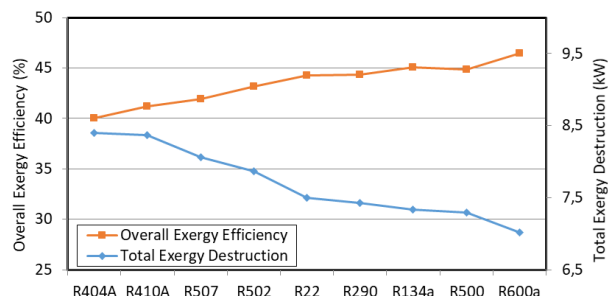


Figure 10. The variation of overall exergy efficiency and total exergy destruction values of the ICBAC system according to different refrigerants

Acknowledgements

The authors wish to thank TEMSA for their invaluable contributions to the research.

The author(s) received no financial support for the research, authorship, and/or publication of this article.

Abbreviations

AC	Air Conditioning
MR	air mixing ratio
ODP	ozone depletion potential
HCFC	hydrochlorofluorocarbon
HFC	hydrofluorocarbon
CFC	chlorofluorocarbon
HC	hydrocarbon
CLTD	temperature difference of cooling load
ADP	apparatus Dew Point
SC	shading coefficient
BF	bypass factor
SHGF	solar heat gain factor
COP	Coefficient of Performance
CLTD	Temperature difference of cooling load
GWP	Global-Warming Potential
HAP	Hourly Analysis Program
HVAC	Heating, Ventilating, and Air Conditioning
ICBAC	Inter-City Bus Air Conditioning
MR	Mixing Ratio
ORC	Organic Rankine Cycle

Subscripts

o	outdoor
i	indoor
l	latent
s	sensible
eva	evaporator
con	condenser
comp	compressor
gen	generated
des	destruction
avg	average
rev	reversible

Nomenclature

\dot{Q}	Heat Transfer
U	Total Heat Transfer coefficient
A	Heat Transfer surface area
T	Temperature
T_s	supply air Temperature
T_{ADP}	coil apparatus dew-point Temperature
T_m	mixed air Temperature
T_0	dead state Temperature
W	Work
h	enthalpy

V	velocity
h_{fg}	latent heat of vaporization
c_p	specific heat of moist
w	humidity ratio
\dot{m}	mass flow rate
ex	exergy

Greek

η	efficiency
ψ	exergy efficiency

5. References

1. M. Bilgili, A. Ozbek, B. Sahin, and A. Kahraman, "An overview of renewable electric power capacity and progress in new technologies in the world," *Renew. Sustain. Energy Rev.*, vol. 49, pp. 323–334, Sep. 2015.
2. A. Korompili, Q. Wu, and H. Zhao, "Review of VSC HDC connection for offshore wind power integration," *Renew. Sustain. Energy Rev.*, vol. 59, pp. 1405–1414, Jun. 2016.
3. P. Söderholm and M. Pettersson, "Offshore wind power policy and planning in Sweden," *Energy Policy*, vol. 39, no. 2, pp. 518–525, Feb. 2011.
4. A. Hepbasli, Z. Erbay, F. Icier, N. Colak, and E. Hancioglu, "A review of gas engine driven heat pumps (GEHPs) for residential and industrial applications," *Renewable and Sustainable Energy Reviews*, vol. 13, no. 1, Pergamon, pp. 85–99, 01-Jan-2009.
5. "Energy Technology Perspectives," 2010.
6. I. E. A. IEA, "Technology roadmap, wind energy," 2013.
7. I. E. A. IEA, "Carbon capture and storage, the solution for deep emissions reductions," 2015.
8. M. F. Sukri, M. N. Musa, M. Y. Senawi, and H. Nasution, "Achieving a better energy-efficient automotive air-conditioning system: a review of potential technologies and strategies for vapor compression refrigeration cycle," *Energy Effic.*, vol. 8, no. 6, pp. 1201–1229, Dec. 2015.
9. S. Kobayashi, S. Plotkin, and S. K. Ribeiro, "Energy efficiency technologies for road vehicles," *Energy Effic.*, vol. 2, no. 2, pp. 125–137, May 2009.
10. X. Chen, G. Zhang, Q. Zhang, and H. Chen, "Mass concentrations of BTEX inside air environment of buses in Changsha, China," *Build. Environ.*, vol. 46, no. 2, pp. 421–427, Feb. 2011.
11. K. D. Huang, S.-C. Tzeng, T.-M. Jeng, and W.-D. Chiang, "Air-conditioning system of an intelligent vehicle-cabin," *Appl. Energy*, vol. 83, no. 6, pp. 545–557, Jun. 2006.
12. L. S. Lim and M. O. Abdullah, "Experimental Study of an Automobile Exhaust Heat-Driven Adsorption Air-Conditioning Laboratory Prototype by Using Palm Activated Carbon-Methanol," *HVAC&R Res.*, vol. 16, no. 2, pp. 221–231, Mar. 2010.
13. E. Z. E. Conceicao, M. C. G. Silva, and D. X. Viegas, "Airflow Around a Passenger Seated in a Bus," *HVAC&R Res.*, vol. 3, no. 4, pp. 311–323, Oct. 1997.
14. F. J. Pino, D. Marcos, C. Bordons, and F. Rosa, "Car air-conditioning considerations on hydrogen consumption in fuel cell and driving limitations," *Int. J. Hydrogen Energy*, vol. 40, no. 35, pp. 11696–11703, Sep. 2015.
15. Y. Farzaneh and A. A. Tootoonchi, "Controlling automobile thermal comfort using optimized fuzzy controller," *Appl. Therm. Eng.*, vol. 28, no. 14–15, pp. 1906–1917, Oct. 2008.
16. M. Linder and R. Kulenovic, "An energy-efficient air-conditioning system for hydrogen driven cars," *Int. J. Hydrogen Energy*, vol. 36, no. 4, pp. 3215–3221, Feb. 2011.
17. M. Hegar, M. Kolda, M. Kopecka, V. Rajtmajer, and A. Ryska, "Bus HVAC energy consumption test method based on HVAC unit behavior," *Int. J. Refrig.*, vol. 36, no. 4, pp. 1254–1262, Jun. 2013.
18. N. F. Tumen Ozdil and M. R. Segmen, "Investigation of the effect of the water phase in the evaporator inlet on economic performance for an Organic Rankine Cycle (ORC) based on industrial data," *Appl. Therm. Eng.*, vol. 100, pp. 1042–1051, May 2016.
19. N. F. Tumen Ozdil, A. Tantekin, and Z. Erbay, "Energy and exergy analyses of a fluidized bed coal combustor steam plant in textile industry," *Fuel*, vol. 183, pp. 441–448, Nov. 2016.
20. M. Khamis Mansour, M. N. Musa, M. N. Wan Hassan, and K. M. Saqr, "Development of novel control strategy for multiple circuit, roof top bus air conditioning system in hot

humid countries,” *Energy Convers. Manag.*, vol. 49, no. 6, pp. 1455–1468, Jun. 2008.

21. M. K. Mansour, M. N. Musa, and M. N. W. Hassan, “Thermoeconomic optimization for a finned-tube evaporator configuration of a roof-top bus air-conditioning system,” *Int. J. Energy Res.*, vol. 32, no. 4, pp. 290–305, Mar. 2008.

22. K. W. Shek and W. T. Chan, “Combined comfort model of thermal comfort and air quality on buses in Hong Kong,” *Sci. Total Environ.*, vol. 389, no. 2–3, pp. 277–282, Jan. 2008.

23. M. Direk and M. Hosoz, “Energy and exergy analysis of an Automobile Heat Pump system,” *Int. J. Exergy*, vol. 5, no. 5/6, p. 556, 2008.

24. A. Alkan and M. Hosoz, “Experimental performance of an automobile air conditioning system using a variable capacity compressor for two different types of expansion devices,” *Int. J. Veh. Des.*, vol. 52, no. 1/2/3/4, pp. 160–176, 2010.

25. A. Alkan and M. Hosoz, “Comparative performance of an automotive air conditioning system using fixed and variable capacity compressors,” *Int. J. Refrig.*, vol. 33, no. 3, pp. 487–495, May 2010.

26. C. Schulze, G. Raabe, W. J. Tegethoff, and J. Koehler, “Transient evaluation of a city bus air conditioning system with R-445A as drop-in – From the molecules to the system,” *Int. J. Therm. Sci.*, vol. 96, pp. 355–361, Oct. 2015.

27. Ş. Ünal, “Determination of the ejector dimensions of a bus air-conditioning system using analytical and numerical methods,” *Appl. Therm. Eng.*, vol. 90, pp. 110–119, Nov. 2015.

28. A. Yılmaz, “Transcritical organic Rankine vapor compression refrigeration system for intercity bus air-conditioning using engine exhaust heat,” *Energy*, vol. 82, pp. 1047–1056, Mar. 2015.

29. Ş. Ünal and T. Yılmaz, “Thermodynamic analysis of the two-phase ejector air-conditioning system for buses,” *Appl. Therm. Eng.*, vol. 79, pp. 108–116, Mar. 2015.

30. E. Tosun, M. Bilgili, G. Tuccar, A. Yasar, and K. Aydin, “0,” *Int. J. Exergy*, vol. 20, no. 4, p. 445, 2016.

31. Y. A. Çengel and M. A. Boles,

Thermodynamics : an engineering approach. .

32. M. Bilgili, “Hourly simulation and performance of solar electric-vapor compression refrigeration system,” *Sol. Energy*, vol. 85, no. 11, pp. 2720–2731, Nov. 2011.

33. E. Hürdoğan, O. Büyükalaca, A. Hepbasli, and T. Yılmaz, “Exergetic modeling and experimental performance assessment of a novel desiccant cooling system,” *Energy Build.*, vol. 43, no. 6, pp. 1489–1498, Jun. 2011.

34. Ediz Cardak, “Energy and Exergy Analysis of an Inter-City Bus Air-Conditioning System Working with Different Refrigerants,” Cukurova University, 2017.

35. N. Y. Salih Coşkun, Recep Yamankaradeniz, İlhami Horuz, *İklimlendirme Esasları ve Uygulamaları*. 2015.

36. Thermodynamic Properties of DuPont™ Suva® 404A (HP62) Refrigerant (R-404A) T-404A (HP62)—ENG Units and Factors.”

37. “Technical Guidelines:R404A, 5th. edition, National Refrigerants.” [Online]. Available:

http://www.refrigerants.com/pdf/R404A_LIN K.pdf. [Accessed: 27-Nov-2017].

38. 2010 ASHRAE HANDBOOK - REFRIGERATION, Inch-Pound., vol. 30329, no. 404. Atlanta: American Society of Heating, Refrigerating and Air-Conditioning Engineers, 2010.

39. A. Gencer and D. ˘lu, “Seasonal performance assessment of refrigerants with low GWP as substitutes for R410A in heat pump air conditioning devices,” 2017.

40. Y. Ust, A. S. Karakurt, and U. Gunes, “Performance Analysis of Multipurpose Refrigeration System (MRS) on Fishing Vessel,” *Polish Marit. Res.*, vol. 23, no. 2, pp. 45–56, 2016.

41. S. A. Klein and G. Nellis, *Thermodynamics*, 1st ed. Cambridge University Press, 2012.

42. B. Saleh, “Parametric and working fluid analysis of a combined organic Rankine-vapor compression refrigeration system activated by low-grade thermal energy,” *J. Adv. Res.*, vol. 7, no. 5, pp. 651–660, 2016.

43. 2009 ASHRAE HANDBOOK - FUNDAMENTALS, SI Edition. Atlanta: American Society of Heating, Refrigerating and Air-Conditioning Engineers, 2009.

44. M. S. Owen, Ed., *2014 ASHRAE HANDBOOK - REFRIGERATION*, SI Edition. Atlanta: ASHRAE, 2014.